Characteristics of phonon transmission across epitaxial interfaces: a lattice dynamic study

2007 J. Phys.: Condens. Matter 19 236211

(http://iopscience.iop.org/0953-8984/19/23/236211)

IOP PUBLISHING JOURNAL OF PHYSICS: CONDENSED MATTER

J. Phys.: Condens. Matter **19** (2007) 236211 (13pp) doi:10.1088/0953-8984/19/23/236211

Characteristics of phonon transmission across epitaxial interfaces: a lattice dynamic study

Jian Wang and Jian-Sheng Wang

Center for Computational Science and Engineering and Department of Physics, National University of Singapore, Singapore 117542, Republic of Singapore

Received 7 February 2007, in final form 27 March 2007
Published 11 May 2007
Online at stacks.iop.org/JPhysCM/19/236211

Abstract

Phonon transmission across epitaxial interfaces is studied within the lattice dynamic approach. The transmission shows weak dependence on frequency for a lattice wave with a fixed angle of incidence. The dependence on azimuth angle is found to be related to the symmetry of the boundary interface. The transmission varies smoothly with the change of the incident angle. A critical angle of incidence exists when the phonon is incident from the side with large group velocities to the side with low ones. No significant mode conversion is observed among different acoustic wave branches at the interface, except when the incident angle is near the critical value. Our theoretical result of the Kapitza conductance G_K across the Si–Ge(100) interface at temperature $T = 200$ K is 4.6×10^8 W K^{-1} m^{-2}. A scaling law $G_K \propto T^{2.87}$ at low temperature is also reported. Based on the features of transmission obtained within the lattice dynamic approach, we propose a simplified formula for thermal conductance across the epitaxial interface. A reasonable consistency is found between the calculated values and the experimentally measured ones.

(Some figures in this article are in colour only in the electronic version)

1. Introduction

The interfacial thermal conductance plays a critical role in nanometre-scaled devices [1, 2]. Kapitza resistance [3] was first discovered in the 1940s. Although much work, both theoretical and experimental [1–9], has been done since then, the characteristic behaviour of phonon transmission across the interface is still not clear. The continuum elastic wave model [4] may be inaccurate when the details of atomistic structures and phonon dispersions are considered. The diffusive scattering theory [2] neglects the wave property of phonons. Here we study phonon transmission across interfaces with the lattice dynamic approach [7, 8], which can simulate the phonon transmission across interfaces atomistically from first principles. We concentrate on the phonon transmission at a single epitaxial interface to capture salient features of transmission.

The paper is organized as follows. We first present the method employed in this study. Using this method we calculate the dependence of phonon transmission on frequency, the azimuth angle, the incident angle, the mode conversion at the Si–Ge interface and at the Si–GaP interface in section 3. Some features of phonon transmission are obtained and discussed. Finally, on the basis of these features, we propose a simplified formula for thermal conductance across an interface. A comparison between the calculated thermal conductance and the experimentally measured values is made.

2. Method

We consider the problem of phonon transmission across an epitaxial interface. Two types of important crystal structure in semiconductors, diamond and zinc blende, are chosen in this study. The crystals on each side of the interface are assumed to be semi-infinite [7–9]. For simplicity, we also neglect the defects possibly existing between the two crystal solids and assume that the interface is an ideal epitaxial interface. The lattice dynamic approach also requires that the harmonic approximation for solids is valid. This condition is usually satisfied at low temperatures. For the scattering of waves at interface, we remark that the nonlinear effect may be less important than the elastic scattering at low temperature because the thickness of the boundary area at the interface is smaller than the mean free path of phonons.

We follow the scattering boundary method in [7, 8]. We write the solutions on the incident side and on the transmitted side with the unknown component coefficients expressed as follows. If a normal mode $\tilde{\mathbf{u}}^{\mathrm{L}}_{l,i,n}(\omega, \mathbf{q})$ is incident from the left lead, the scattering solution for the perfect leads can be assumed as

$$\mathbf{u}^{\mathrm{L}}_{l,i} = \tilde{\mathbf{u}}^{\mathrm{L}}_{l,i,n}(\omega, \mathbf{q}_n) + \sum_{n'} t^{\mathrm{LL}}_{n'n} \tilde{\mathbf{u}}^{\mathrm{L}}_{l,i,n'}(\omega, \mathbf{q}'_{n'}), \tag{1a}$$

$$\mathbf{u}^{\mathrm{R}}_{l,i} = \sum_{n''} t^{\mathrm{RL}}_{n''n} \tilde{\mathbf{u}}^{\mathrm{R}}_{l,i,n''}(\omega, \mathbf{q}''_{n''}), \tag{1b}$$

where i, l denote the ith atom in the l unit cell, and n, n' and n'' refer to the different polarized branches of incident, reflected and transmitted waves. Frequency is denoted as ω. Wavevectors for the incident, reflected, and transmitted waves are $\mathbf{q}$, $\mathbf{q}'$, and $\mathbf{q}''$, respectively. The superscripts L and R indicate left and right. In these equations, $t^{\mathrm{RL}}_{n''n}$ and $t^{\mathrm{LL}}_{n'n}$ are the amplitude transmission/reflection coefficients from mode n on the lead L to mode n'' on lead R, and to mode n' on lead L. The wavevectors $\mathbf{q}'$ and $\mathbf{q}''$ satisfy $\omega = \omega_{n'}(\mathbf{q}') = \omega_{n''}(\mathbf{q}'')$. Note that frequency does not change because the system is linear.

In this paper, we consider the phonon transmission across two types of epitaxial interface: the interface between silicon and germanium and the interface between silicon and gallium phosphide. Now the problem is to determine the wavenumbers for the possible branches of the reflected and the transmitted waves. Since the system is homogeneous in the x and y directions, the transverse components of the wavevector for the reflected waves $\mathbf{q}'$ and for the transmitted waves $\mathbf{q}''$ have the same values as that of the incident wave $\mathbf{q}$, that is $q'_x = q''_x = q_x$; $q'_y = q''_y = q_y$. The longitudinal components, q'_z and q''_z, satisfy $\omega(\mathbf{q}) = \omega(\mathbf{q}') = \omega(\mathbf{q}'')$. We solve the nonlinear equation to find q'_z or q''_z for the (111) interface with the numerical method in [10]. For the (100) interface, we utilize a more efficient eigenvalue method to obtain the solutions of nonlinear equations [9]. The wavevectors q'_z and q''_z are identified from these solutions to satisfy the following conditions:

(i) the reflected waves should have negative group velocity $v_z(\mathbf{q}')$, so that the phonon energy of the reflected waves will propagate back to the $-z$ direction;

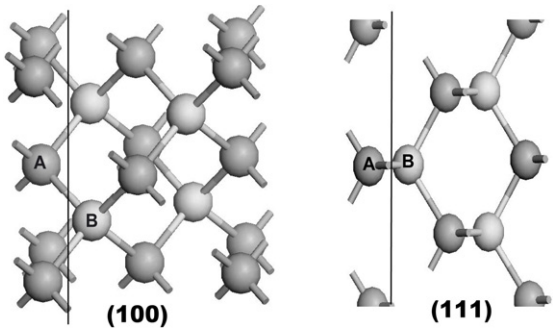

Figure 1. Atomic interfacial structure of the (100) and (111) interfaces.

(ii) the transmitted wave should have positive group velocity so that the phonon energy of the transmitted waves will propagate to the $+z$ direction;

(iii) when the wavenumbers for the reflected and transmitted waves are complex, they are identified from the solutions to satisfy $\mathbf{Im}(q_z') < 0$ and $\mathbf{Im}(q_z'') > 0$, so that these waves decay in space.

Actually these decay waves with complex wavenumber do not propagate any energy and the phase difference along the z direction for atoms in the neighbouring unit cells is π. But they are physically possible modes at the interface and must be considered in the scattering boundary method.

Now we consider the dynamic equations for atoms at the interface. The (100) and (111) interfaces between the diamond structure or the zinc blende structure is illustrated in figure 1. We assume that the transverse directions at the interface are infinitely large so that the boundary atoms on each side, e.g., A atoms in the figure, are translationally invariant. The dynamic equations for A position atoms are equivalent, and similarly for B position atoms on the other side of the interface. So we only need to consider the dynamic equations for atom A and for atom B at the interface. Under the harmonic approximation, these dynamic equations at a given frequency ω can be written as $-m_i\omega^2\mathbf{u}_i + \sum_j \mathbf{K}_{i,j} \cdot \mathbf{u}_j = 0$, where m_i denotes the atomic mass for each atom, $\mathbf{u}_i$ is the oscillation amplitude and the $\mathbf{K}_{i,j}$ are force constants. The force constants across the interface are chosen as the symmetrized $K_{ij} = (K_{ij}^{\mathrm{L}} + K_{ij}^{\mathrm{R}})/2$. After substituting equation (1) into this dynamic equation, we get six equations with six unknown coefficients. This system of equations can be solved by a conventional method. The energy transmission from mode (L, n) to mode (R, n'') is given by

$$\tilde{T}_{n''n}^{\mathrm{RL}} = |t_{n''n}^{\mathrm{RL}}|^2 \frac{\tilde{v}_{n''}^{\mathrm{R}}}{\tilde{v}_n^{\mathrm{L}}}. \tag{2}$$

Here $\tilde{v}_n^{\mathrm{L}}$ is the reduced group velocity [8] along the z direction for mode n in the left lead, defined by $\tilde{v}_n^{\mathrm{L}} = v_n^{\mathrm{L}}/l_{\mathrm{L}}$, where v_n^{L} is the group velocity and l_{L} is the lattice constant for the left lead. Similar meaning holds for $\tilde{v}_n^{\mathrm{R}}$. The total reflection $\mathcal{R}_n^{\mathrm{L}}$ and transmission coefficients $\mathcal{T}_n^{\mathrm{L}}$ for (L, n) are given, respectively, by

$$\mathcal{R}_n^{\mathrm{L}} = \sum_{n'} |t_{n'n}^{\mathrm{LL}}|^2 \frac{\tilde{v}_{n'}^{\mathrm{L}}}{\tilde{v}_n^{\mathrm{L}}}, \qquad \mathcal{T}_n^{\mathrm{L}} = \sum_{n''} |t_{n''n}^{\mathrm{RL}}|^2 \frac{\tilde{v}_{n''}^{\mathrm{R}}}{\tilde{v}_n^{\mathrm{L}}}, \tag{3a}$$

$$\mathcal{R}_n^{\mathrm{L}} + \mathcal{T}_n^{\mathrm{L}} \equiv 1. \tag{3b}$$

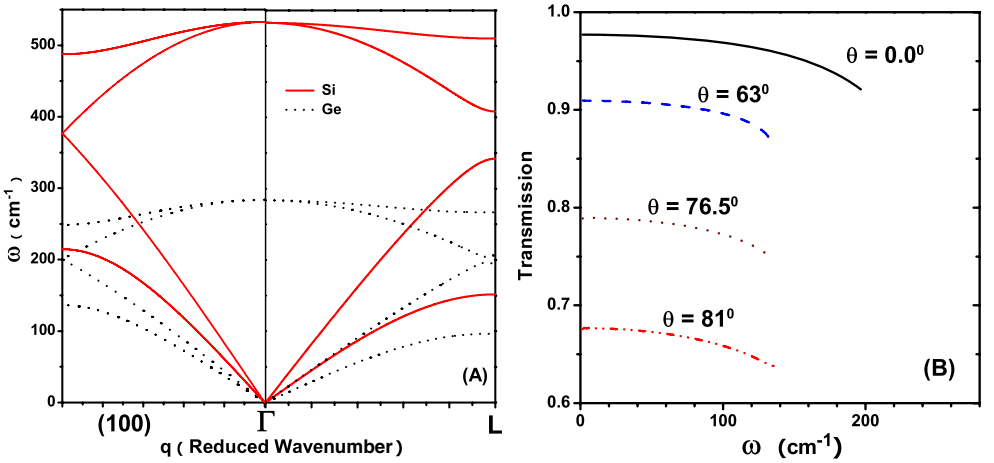

Figure 2. (A) Phonon dispersion for Si and Ge along Γ–L and the [100] direction. (B) The energy transmission $T_n(\omega)$ as a function of frequency ω across the Si–Ge(100) interface for LA waves at different angles of incidence from Si to Ge.

The group velocity along the z direction is calculated through the dynamic matrix as

$$v_z = \frac{1}{2\omega} \frac{\tilde{\mathbf{e}}^\dagger \frac{\partial \mathbf{D}}{\partial q_z} \tilde{\mathbf{e}}}{\tilde{\mathbf{e}}^\dagger \cdot \tilde{\mathbf{e}}}, \tag{4}$$

where $\mathbf{D}$ is the dynamic matrix and $\tilde{\mathbf{e}}$ the eigenvector of the dynamic matrix [8]. Note that the energy conservation relation, equation (3*b*), is satisfied automatically. This can be used as a check. With the relation equation (3), we can get the Kapitza conductance G_K as

$$G_K = \frac{1}{V} \sum_{\mathbf{q},n} \hbar\omega_n(\mathbf{q}) v_n^z(\mathbf{q}) \mathcal{T}_n(\mathbf{q}, \omega_n) \frac{\partial f(\omega_n, T)}{\partial T}, \tag{5}$$

where $\mathcal{T}_n(\mathbf{q}, \omega_n)$ is the transmission [8] calculated from equation (3), V is the volume and $f(\omega_n, T)$ is the Bose–Einstein distribution for the nth branch mode. When using equation (5), we compute the Kapitza conductance from the Si side. The lattice constant for the conventional Si unit cell is $a = 5.43$ Å.

3. Models and numerical results

In this section, we report the dependence of phonon transmission on the frequency, azimuth angle, and incident angle across the Si and Ge interface. We then consider the mode conversion problem at the interface. Phonon transmission across a kind of zinc blende interface, Si–GaP, is also studied to investigate the lattice structure effect on transmission.

The atomic masses for Si and Ge are 28 and 72.61 amu, respectively. After optimizing the structure using the Tersoff potential [11], we obtain the linearized force constants under small displacement. Due to the Tersoff potential truncation function, [11], only the four nearest atoms need to be considered for each atom. The phonon dispersions for the Si and Ge along the Γ–L direction can be calculated through the linearized force constants from the dynamic matrix, and they are illustrated in figure 2. The maximum frequency of the longitudinal acoustic (LA) branch along Γ–L for Si and Ge is 343 and 196 cm^{-1}, respectively. Compared with the experimental Si and Ge phonon dispersions [12], there is a discrepancy between the calculated

phonon frequency in figure 2 and the experimental values. This inaccuracy comes from the lack of more neighbouring atoms for Tersoff potential, apart from the first neighbouring ones. The *ab initio* method [13], which can include higher-order neighbouring atoms, is desirable for the more elaborate phonon dispersion relations. However, we find that the inclusion of higher-order neighbouring atoms will make the calculation of energy transmission very difficult because the solutions of q_z' or q_z'' at a given frequency ω is rather complicated. We estimate that such errors of phonon dispersion relation in the Brillouin boundary will not have much influence on the energy transmission across the interface. The force constants from the first neighbouring atoms play a main role in the computation of phonon dispersion relations. The cut-off frequency of energy transmission across the interface will not approach closely to the boundaries of the Brillouin boundary apart from a few high-symmetry directions. The transmission decreases very rapidly when the frequency is near cut-off, which can be seen from figure 2(B). Therefore, we think that the inaccuracy of the Brillouin boundary values from Tersoff potential will not significantly change the results of energy transmission across the interface.

3.1. Dependence on angular frequency

The transmission's dependence on angular frequency across a (100) Si–Ge interface is shown in figure 2(B). The incident acoustic wave is longitudinally polarized with an incident angle θ in the xz plane. For waves with incident angle θ below about 63°, the transmission falls into a very narrow range approximately from 0.91 to 0.98, and it decreases slightly with the increase of frequency before it reaches its cut-off frequency. Here the cut-off frequency means that beyond this point the phonon transmission equals zero. There is an abrupt decrease in phonon transmission when the frequency is near this value. When the incident wave is normal to the interface along the [100] direction from Si to Ge, the transmitted waves are also along the [100] direction. Thus, the cut-off frequency of transmission can be easily determined from the phonon dispersion of Ge. This can be shown from figure 2(B). The cut-off frequency is about 197 cm^{-1} for the wave with incident angle $\theta = 0°$, while the endpoint frequency of the longitudinal acoustic wave branch for Ge along the [100] direction is 200 cm^{-1}, which agrees with the cut-off frequency of transmission for the normal incident wave. In figure 2(B), for clarity, we only plot the transmission before its abrupt jump to zero. For transversely polarized incident acoustic waves, we also have observed a similar phenomenon. It can be concluded that the acoustic phonon transmission from Si to Ge varies in a narrow range with the increase of frequency, independent of the property of its polarization. Note that the phonon wave is incident from the material (Si) with a larger group velocity to the material (Ge) with a smaller group velocity. This conclusion also holds in our calculations of the transmissions for other incident acoustic waves, not only in the xz-plane, but also with azimuth angle φ. We remark that this small change of phonon transmission with frequency for an incident wave at the incident angle θ can be neglected for an approximate estimation of thermal conductance across an interface.

3.2. Spatial angular dependence

3.2.1. Azimuth angle and symmetry of the interface. We find that the phonon transmission's dependence on the azimuth angle of the incident wave is related to the symmetry of the interface. The results of the transmissions for the longitudinal acoustic waves incident from Si to Ge are shown in figure 3. It can be seen from figure 3 that the phonon transmission shows little dependence on the azimuth angle φ at incident angle $\theta < 45°$ for both the (100) and (111) interfaces. However, when the incident angle increases beyond 45°, there are peaks in transmission with the variation of the azimuth angle. The peaks reveal the anisotropy of

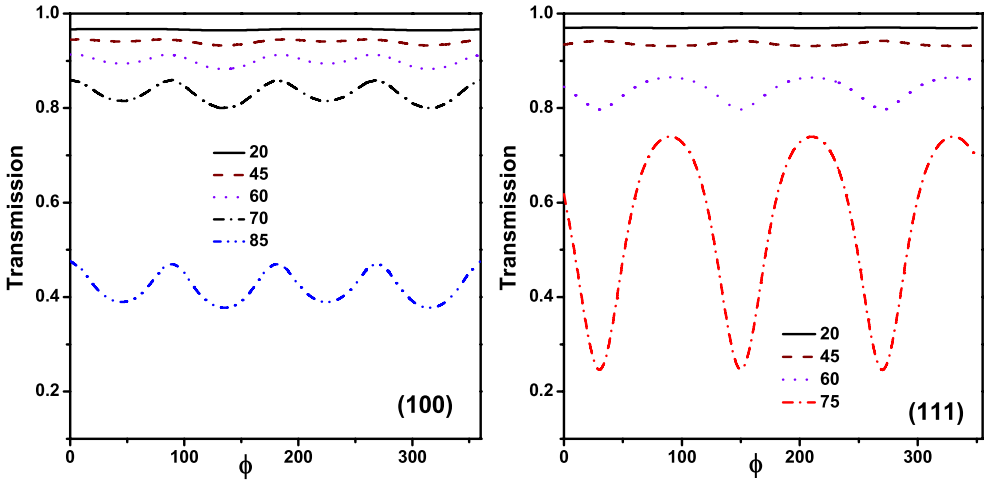

Figure 3. Dependence of the longitudinal acoustic phonon transmission on the azimuth angle φ. All transmissions plotted are at angular frequency $\omega = 15\ \mathrm{cm}^{-1}$ and are incident from Si to Ge. Different lines in the figure correspond to the transmissions for wave with different incident angle θ as the indicated in the figure. The left figure shows the results for the (100) interface, and the right figure for the (111) interface.

the interface. There is a four-fold symmetry axis in the [100] direction in Si or Ge and a three-fold symmetry axis along the [111] direction. These symmetries have evidently been shown in the phonon transmission across the related interface. In figure 3, there are four-fold symmetrical peaks separated by $\pi/2$ in the transmission across the (100) interface. Three three-fold symmetrical peaks separated by $2\pi/3$ appear in the transmission across the (111) interface.

3.2.2. Critical incident angle. We next report the result of the dependence of energy transmission on the incident angle. A continuum wave incident on a surface with an incident angle θ is refracted in accordance with Snell's law. It would be an interesting question to ask if there is a critical angle for discrete lattice waves. We calculated the phonon transmission incident from Si to Ge and incident from Ge to Si. The dependence of transmission on the incident angle is illustrated in figure 4 for the (100) Si–Ge interface.

It can be seen from figure 4 that when the angle θ for the phonon incident from Si to Ge increases, energy transmission decreases slowly. The incident angle from Si to Ge can be extended to as large as 90°. In contrast to the transmission from Si to Ge, for waves incident from Ge to Si, there exists a critical angle, about 38° for LA waves and 38.5° for TA waves, above which the transmission is very small. We can estimate the critical angle with the help of Snell's law for a continuum wave. The group velocities calculated from the dynamic matrix in this paper for longitudinally polarized waves along the [001] direction are $v_{\mathrm{L}}^{\mathrm{Si}} \approx 6.87\ \mathrm{km\ s}^{-1}$ and $v_{\mathrm{L}}^{\mathrm{Ge}} \approx 3.78\ \mathrm{km\ s}^{-1}$, respectively. Snell's law in the continuum wave model gives the critical angle $\theta_{\mathrm{c}} = \sin^{-1}(v_{\mathrm{L}}^{\mathrm{Ge}}/v_{\mathrm{L}}^{\mathrm{Si}}) = 33.4°$ from Ge to Si. This value is a little lower than the observed critical angle value. However, we can still assume that Snell's law holds approximately.

When the incident waves from Si to Ge and from Ge to Si are both normal to the surface ($\theta = 0$), the transmissions from both sides are 0.98 for LA waves and 0.95 for TA waves. We use the acoustic mismatch model [4] to estimate $4Z_{\mathrm{Si}}Z_{\mathrm{Ge}}/(Z_{\mathrm{Si}} + Z_{\mathrm{Ge}})^2 \approx 0.97$ for LA waves,

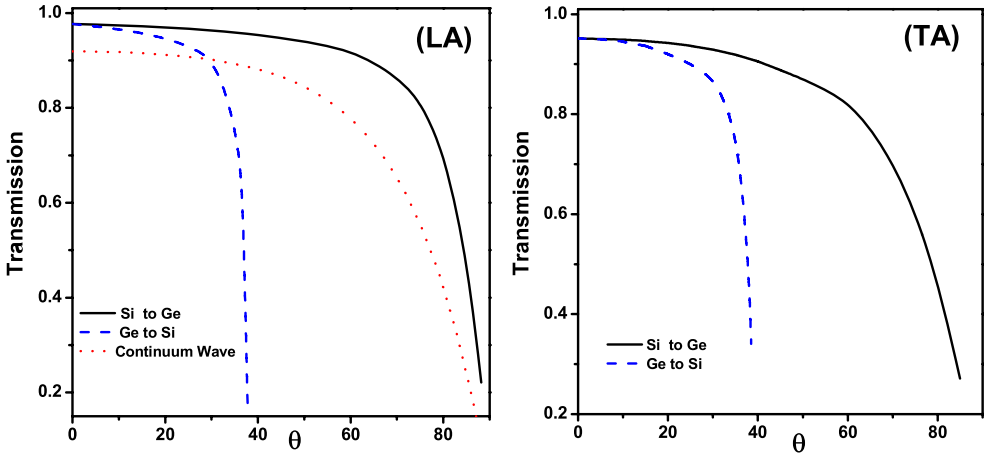

Figure 4. Dependence of phonon transmission on the incident angle θ. The left figure shows the results of longitudinal acoustic (LA) waves and the right figure is for the transverse polarized (TA) waves. The solid lines indicate the transmission from Si to Ge and the dashed lines denote the transmission from Ge to Si. All the transmissions by the lattice dynamic approach are calculated at angular frequency $\omega = 15\ \mathrm{cm}^{-1}$. The dotted line in the left figure is the result calculated from the continuum wave model.

and 0.94 for TA waves, where Z_{Si} and Z_{Ge} denote the acoustic impedance defined as $Z = \rho v$. Here ρ is the mass density and v is the group velocity. Here we take $\rho_{\mathrm{Si}} = 2.329 \times 10^3\ \mathrm{km\ s}^{-1}$ and $\rho_{\mathrm{Ge}} = 5.323 \times 10^3\ \mathrm{km\ s}^{-1}$. The values of group velocities for LA waves are given in the previous paragraph. It can be seen that the acoustic mismatch model in [4] well describes the transmission for normal incident waves.

To investigate the difference in the transmission on the incident angle between the lattice dynamic approach and the continuum wave model, we also calculated the energy transmission of the continuum wave [14]. The results for the Si–Ge interface is illustrated in figure 4. The procedure of calculation is as follows. First, the amplitude transmission [14] is computed from the Fresnel equation $t = \frac{2z\cos\theta}{z\cos\theta + z'\cos\theta'}$, where $z = \sqrt{\rho c}$ and $z' = \sqrt{\rho' c'}$ are the wave impedances for the incident and refraction crystal. Here the mass density ρ and ρ' take the value in the preceding paragraph. The stiffness constants c, c' are $0.796, 0.680 \times 10^{11}\ \mathrm{N\ m}^{-2}$, respectively. The angle of incidence θ and the angle of transmission θ' satisfy Snell's Law. The energy transmission for the continuum wave is calculated through the formula $\mathcal{T} = |t|^2 \frac{\rho' v' \cos\theta'}{\rho v \cos\theta}$, where $v = 8.43\ \mathrm{km\ s}^{-1}$, $v' = 4.87\ \mathrm{km\ s}^{-1}$ are the group velocities for the incident and refraction continuum waves. It can be seen that the isotropic continuum wave gives a similar dependence of transmission of the incident angle. The result for the continuum wave is close to the result of lattices wave.

3.3. Mode conversion at the interface

The mode conversion at the interface would be an interesting problem to pursue. There are two types of mode conversion for thermal transmission across the boundary: acoustic–optical (AO) and acoustic–acoustic (AA). We neglect the optical–optical conversion because the corresponding frequencies do not overlap in our model. We think that this optical–optical conversion's contribution to thermal transport is trivial because of its relatively low group velocity and high energy.

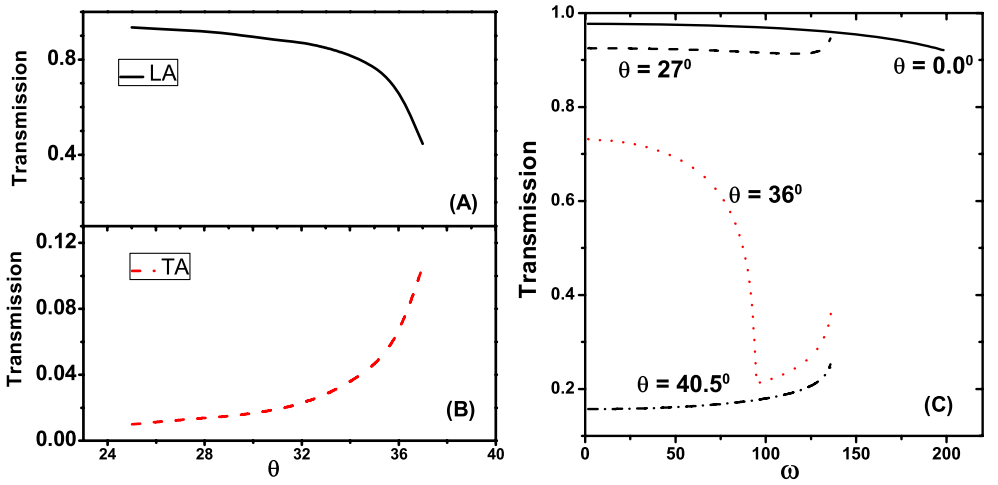

Figure 5. Demonstration of mode conversion LA → LA + TA near the critical angle from Ge to Si. (A) The transmission converted to LA; (B) the transmission to TA; (C) the energy transmission $T_n(\omega)$ as a function of angular frequency ω across the Ge–Si(100) interface for LA waves at different angles of incidence from Ge to Si.

AO conversion. We did not observe significant AO conversion in our simulation of phonon transmission at the Si–Ge interface. The AO conversions in our results are very small, no more than 10%, and they fall in a very narrow frequency range. This result is different from the reported results in [9]. We think that this may come from the empirical potential chosen in our paper, which results in different group velocities. To estimate the maximum ratio of a possible acoustic–optical mode conversion, a simplified 1D toy chain model [8] can be composed because it can be assumed that the AO conversion will be easier for both longitudinal waves in one dimension. However, the results in [8] find that the energy transmission contributed by the AO conversion is trivial in comparison with the acoustic–acoustic transmission. This is due to the large mismatch in their group velocities.

AA conversion. Apart from the possible AO conversion, there are several different polarized acoustic branches. Can the conversion among these different acoustic branches occur at the interface? Our simulation did not find significant conversion among these different polarized branches, except when the angle of incidence is near the critical angle. The reflected and transmitted waves are both LA waves when the incident wave is longitudinally polarized. The same is true for the TA wave. The AA conversion among different polarized acoustic branches only takes place when the angle of incidence is close to the critical angle for waves incident from Ge to Si. Figure 5 shows the transmission of a longitudinally polarized wave incident from Ge to Si. The mode conversion of LA → LA + TA is shown in parts (A) and (B) in figure 5. It can seen that the ratio converted from LA to LA decreases with the increase of the angle of incidence. The ratio converted from LA to TA increases rapidly to about 0.12 near the critical angle. This behaviour of mode conversion taking place near the critical angle may result from the suppression of transmission due to Snell's law. We also find that the presence of the possible reflected waves influences the transmission. For example, in contrast to the transmission from Si to Ge, the dependence of LA mode wave transmission on frequency from Ge to Si shows a rich character, as illustrated in figure 5. For a wave with incident angle $\theta \neq 0$, the transmission

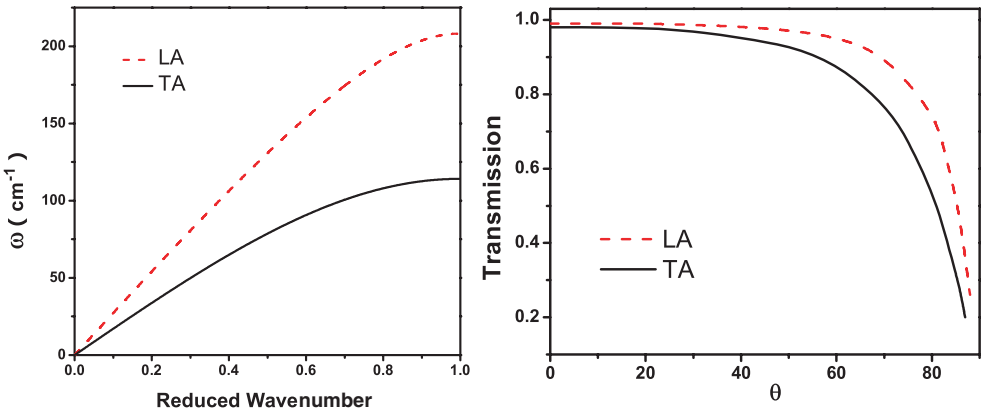

Figure 6. Left figure: phonon dispersion for acoustic waves in GaP. Right figure: dependence of phonon transmission for LA waves on the incident angle θ at angular frequency $\omega = 15$ cm^{-1} from Si to GaP.

first decreases with the increase of frequency. But when the frequency goes over a certain value, for example $\omega = 93$ cm^{-1} for $\theta = 36°$, the transmission begins to increase. This behaviour can be understood by the mode conversion at the interface. It can be seen from figure 2 that the maximum frequency for TA modes in Ge is about 98 cm^{-1}. When the frequency is below this value, there are TA modes for the reflected wave; but over this value, the reflected wave cannot be converted into TA modes. The transmission increases due to lack of reflected modes.

3.4. Transmission across the interface between diamond and zinc blende structures

During the calculation of the transmission of the Si–Ge interface, the atomic masses are uniformly distributed for both Si and Ge on each side. There is another important type of lattice structure in the semiconductor materials. That is the zinc blende structure, where the atomic masses in the sublattice are different. Here we consider an example of gallium phosphide (GaP). To simplify the problem, we only consider the valence force and neglect the Coulomb interaction between the charges when computing the phonon dispersion of GaP. This is a valid approximation when we consider the acoustic phonons that play a major role in the phonon transmission across the interface. The calculated acoustic phonon dispersion curves along Γ–L for GaP are plotted in figure 6. The endpoint values of frequencies along Γ–L for LA and TA waves are about 208 and 116 cm^{-1}, respectively. It can be seen that valence-force constants approximately describe the acoustic branches [15] of GaP. The results of phonon transmission for LA and TA modes across a Si–GaP interface are illustrated in figure 6. We find a consistent dependence on frequency, spatial angular and a similar phenomena of mode conversion with that of the Si–Ge interface. The dependence of transmission on the angle of incidence is illustrated in figure 6.

3.5. Temperature dependence of Kapitza conductance

The Kapitza conductance with the change of temperature is calculated using equation (5), and is illustrated in figure 7(A). The Kapitza conductance for the Si–Ge(100) interface calculated from our model is $G_K = 4.6 \times 10^8$ W K^{-1} m^{-2} when $T = 200$ K. When the temperature goes beyond 200 K, we find that the Kapitza conductance changes little with the temperature and is saturated. For comparison, we plotted the heat capacity of Si in figure 7(B). It can be

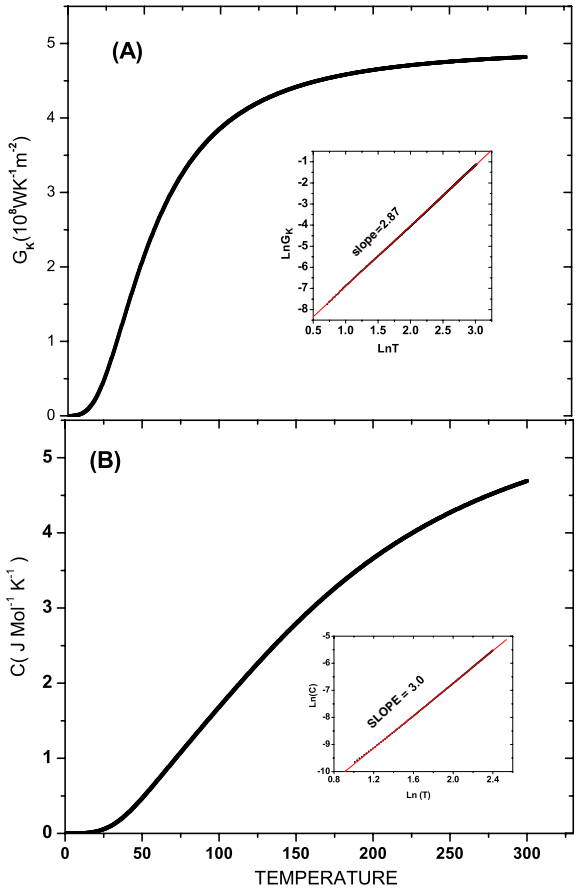

Figure 7. (A) The temperature dependence of Kapitza conductance for the Si–Ge(100) interface. (B) The corresponding heat capacity of Si.

seen that the heat capacity continues to increase with the temperature when $T > 200$ K. In comparison with the heat capacity, the saturation of Kapitza conductance can be accounted for by the negligible contribution of energy transmission from high frequency at low temperatures, as illustrated in the inset of figure 7. The Kapitza conductance scales as $T^{2.87}$, while the heat capacity scales as T^3 in accordance with the Debye model. We have sampled enough points in the first Brillouin zone to ensure that the Kapitza conductance and heat capacity converge numerically. However, due to the small deviation from the value of 3, we cannot rule out the possibility that the exponent for Kapitza conduction is also 3. Reference [7] reported that the Kapitza conductance scaled as T^3 at low temperature for an fcc interface irrespective of the properties for the left and right leads. The temperature dependence of Kapitza conductance is an intriguing problem [2], though much experimental work has been done on this field. Most experiments gave T^α with $\alpha \leqslant 3$ for a solid interface, as reviewed in [2]. So far no experiment result is available for the temperature dependence for the Si–Ge interface. Compared with the results of reference [7] our discrepancy from T^3 comes from the anisotropy of the energy transmission because of the diamond structure used for calculation of the transmission, while reference [7] took an isotropic assumption for their calculation.

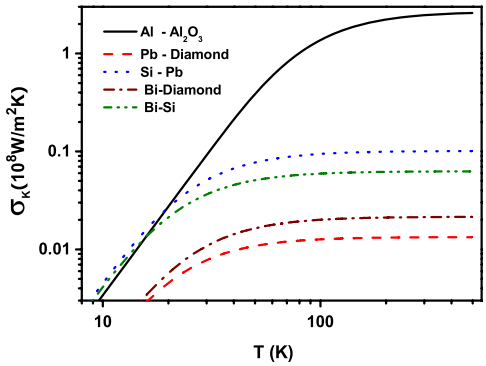

Figure 8. The temperature dependence of Kapitza conductance calculated from equation (7).

4. A new simplified approximate formula

To get a simplified expression, we make the follow approximation on the basis of the features of transmission discussed above. (1) For transmission with a given incident angle θ, we assume that it is independent of the frequency. (2) We neglect the dependence on the azimuth angle. (3) The conductance can be calculated from either the left or the right side [8]. They give the same result across the interface. It is found that the transmission from the high group velocity to the low velocity side has a simpler feature. We calculate the transmission from the high to the low velocity side. The dependence of transmission on the incident angle for a polarized waves is formulated as $\mathcal{T}^n = \mathcal{T}_0^n \cos\theta$. Here $\mathcal{T}_0^n$ is the transmission at $\omega = 0$ with the angle of incidence $\theta = 0$, and is given by

$$\mathcal{T}_0^n = \frac{4Z_1^n Z_2^n}{(Z_1^n + Z_2^n)^2} \tag{6a}$$

$$Z_i^n = \rho_i \frac{v_i^n}{l_i}, \qquad \text{with } i = 1, 2. \tag{6b}$$

Here Z_i^n is the acoustic impedance for the polarized wave and l_i is the lattice constant. We have incorporated the effect of difference in lattice constants of the crystal. It can be seen from figure 4 that the cosine function is a valid approximation. (4) Mode conversion at the interface can be neglected. (5) Since thermal conductance is contributed mainly by acoustic waves, we can assume that the upper limit of frequency of acoustic waves is characterized by the Debye temperature of the side with the low group velocity. A linear dependence of phonon dispersion relation $\omega = q v_n$ is used because thermal conductance is mainly due to acoustic waves. The group velocity v_n^z along z in equation (5) is given by $v_n^z = v_n \cos\theta$. Under these conditions, we have a simplified thermal conductance (Kapitza conductance) as

$$\sigma_{\mathrm{K}} = \frac{1}{12\pi^2} \sum_n \frac{\mathcal{T}_0^n}{v_n^2} \frac{k_{\mathrm{B}}^4 T^3}{\hbar^3} \int_0^{x_{\mathrm{D}}} \frac{x^4 \mathrm{e}^x}{(\mathrm{e}^x - 1)^2} \,\mathrm{d}x. \tag{7}$$

Here v_n is the group velocity of the incident side with the large group velocity. The upper limit x_{D} is given as $x_{\mathrm{D}} = \frac{\theta_{\mathrm{D}}}{T}$, where θ_{D} is the Debye temperature for the other side with low group velocity. We use equation (7) to calculate a few interfaces across which the experimentally measured thermal conductance is available. The parameters taken are shown in table 1. The results of calculation are shown in figure 8.

We list the experimental values and our calculated values in table 2. It can be seen that the calculated values are consistent with the experimental values except for the interface

Table 1. Values for mass density ρ, lattice constant l, the longitudinal group velocity v_L, the transversal group velocities v_T, heat capacity C_v and the Debye temperature θ_D. These values are from [2, 16, 17].

	ρ (10^3 kg m^{-3})	l (Å)	v_L (km s^{-1})	v_T (km s^{-1})	C_v (10^6 J m^{-2} K^{-1})	θ_D (K)
Si	2.329	5.43	8.43	5.84	1.63	640
Al	2.699	4.05	6.24	3.04	2.42	394
Al_2O_3	3.97	4.76	10.89	6.45	2.656	1024
Bi	9.79	4.75	1.972	1.074	1.194	120
Pb	11.598	4.95	2.35	0.97	1.463	105
Diamond	3.515	3.57	17.52	12.82	1.8278	1860

Table 2. Comparison of thermal conductance across interface for the experimental measured values and the calculated values at $T = 200$ K. The experimental values are from [6]. The values are in the units of 10^8 W m^{-2} K^{-1}.

	Al/Al_2O_3	Pb/diamond	Bi/diamond	Pb/Si	Bi/Si
Exp. values	1.2	0.125	0.06	0.13	0.1025
Cal. values	2.5	0.013	0.02	0.10	0.0640

Pb/diamond. The large deviation for the Pb/diamond interface between the calculated and experimental values may come from the nonlinear scattering effect at the interface. It cannot be explained by the method employed in this paper.

5. Discussion and conclusion

We have studied the features of phonon transmission across the epitaxial interfaces by the lattice dynamic approach. The transmission is found to change slightly with the frequency for polarized waves with a given incident angle from the high group velocity side to the low group velocity side. The dependence of transmission on the azimuth angle is related to the symmetrical properties of the interface for waves with larger angle of incidence. A critical angle exists for transmissions from the low group velocity side to the higher group velocity side. The dependence of transmission on the mode conversion at the interface is trivial except when the incident angle is close to the critical angle. Thermal conductance across the epitaxial interfaces is dominantly contributed by the acoustic waves and is insensitive to the mass distribution of different lattice positions. Kapitza conductance across the Si–Ge(100) interface shows a $T^{2.87}$ dependence on temperature, which is very close to T^3 behaviour. A simplified formula for the estimation of thermal conductance across the interface is proposed in the light of features found by the lattice dynamic approach. We remark that this formula can give a valid estimation of Kapitza conductance across solid epitaxial interfaces when nonlinear phonon scattering is unimportant. We think nonlinear scattering sometimes may be important for the interfaces between materials with a large disparity in values of the Debye temperature, such as Pb/diamond. Such a nonlinear effect cannot be captured in the current lattice dynamic approach. From the calculation, the nonlinear effect may contribute to the increase of thermal conductance across the solid interface by breaking the selection rules between the linear phonon dispersion relations. The phase relations among the incident wave and the reflected, transmitted waves have not been considered because they will not influence the energy transmission across the interface. A possible existence of lattice dislocation or disorder is not included in the present lattice dynamic approach.

Acknowledgments

We think Dr Jingtao Lü for a careful reading of the manuscript. This work is supported in part by a Faculty Research Grant of the National University of Singapore.

References

[1] Cahill D G *et al* 2003 *J. Appl. Phys.* **93** 793
[2] Swartz E T and Pohl R O 1989 *Rev. Mod. Phys.* **61** 605
[3] Kapitza P L 1941 *Can. J. Phys.* **4** 181
[4] Little W A 1959 *Can. J. Phys.* **37** 334
[5] Chen G 1998 *Phys. Rev.* B **57** 14958
[6] Costescu R M, Wall M A and Cahill D G 2003 *Phys. Rev.* B **67** 054302
Lyeo H-K and Cahill D G 2006 *Phys. Rev.* B **73** 144301
[7] Young D A and Maris H J 1989 *Phys. Rev.* B **40** 3685
Stoner R J and Maris H J 1993 *Phys. Rev.* B **48** 16373
[8] Wang J and Wang J-S 2006 *Phys. Rev.* B **74** 054303
[9] Zhao H and Freund J B 2005 *J. Appl. Phys.* **97** 024903
Zhao H and Freund J B 2005 *J. Appl. Phys.* **97** 109901
[10] Press W H *et al* 2002 *Numerical Recipes in C* 2nd edn (Cambridge: Cambridge University Press) p 59
[11] Brenner D W *et al* 2002 *J. Phys.: Condens. Matter* **14** 783
Tersoff J 1989 *Phys. Rev.* B **39** 5566
[12] Tubino R, Piseri L and Zerbi G 1972 *J. Chem. Phys.* **56** 1022
Giannozzi *et al* 1991 *Phys. Rev.* B **43** 7231
[13] Parlinski K, Li Z Q and Kawazoe Y 1997 *Phys. Rev. Lett.* **78** 4063
[14] Auld B A 1990 *Acoustic Fields and Waves in Solids* 2nd edn, vol II, ed E Robert (Malabar, FL: Krieger) p 22
[15] Banerjee R and Varshni Y P 1971 *J. Phys. Soc. Japan* **30** 1015
Kane E O 1985 *Phys. Rev.* B **31** 7865
[16] Krenzer B, Janzen A, Zhou P, Linde D and Hoegen M H 2006 *New J. Phys.* **8** 190
[17] Kittel C *et al* 1996 *Introduction to Solid State Physics* 7th edn (New York: Wiley)